

Effects of fermionic dark matter on properties of neutron stars

Qian-Fei Xiang^{1,2}, Wei-Zhou Jiang^{1,3,4*}, Dong-Rui Zhang¹, and Rong-Yao Yang¹

¹ *Department of Physics, Southeast University, Nanjing 211189, China*

² *Institute of High Energy Physics, Chinese Academy of Sciences, Beijing 100049, China*

³ *National Laboratory of Heavy Ion Accelerator, Lanzhou 730000, China*

⁴ *Department of Physics and Santa Cruz Institute for Particle Physics,
University of California, Santa Cruz, CA 95064, USA*

By assuming that only gravitation exists between dark matter (DM) and normal matter (NM), we study the effects of fermionic DM on the properties of neutron stars using the two-fluid Tolman-Oppenheimer-Volkoff formalism. It is found that the mass-radius relationship of the DM admixed neutron stars (DANSs) depends sensitively on the mass of DM candidates, the amount of DM, and interactions among DM candidates. The existence of DM in DANSs results in a spread of mass-radius relationships that cannot be interpreted with a unique equilibrium sequence. In some cases, the DM distribution can surpass the NM distribution to form DM halo. In particular, it is favorable to form an explicit DM halo, provided the repulsion of DM exists. It is interesting to find that the difference in particle number density distributions in DANSs and consequently in star radii caused by various density dependencies of nuclear symmetry energy tends to disappear as long as the repulsion of accumulated DM is sufficient. These phenomena indicate that the admixture of DM in neutron stars can significantly affect the astrophysical extraction of nuclear equation of state by virtue of neutron star measurements. In addition, the effect of the DM admixture on the star maximum mass is also investigated.

PACS numbers: 95.35.+d, 97.60.Jd, 26.60.Kp, 21.60.Jz

I. INTRODUCTION

Nowadays, dark matter (DM) becomes a very hot topic in both astrophysics [1] and particle physics [2], and it seems clear that it is the dominant matter in the universe. Recent advances in cosmological precision tests further consolidate the minimal cosmological standard model, indicating that the universe contains 4.9% ordinary matter, 26.8% DM, and 68.3% dark energy [3]. However, the properties of DM, including its mass and interactions, are still unknown. It is thus of great interest to explore the properties of DM through direct or indirect methods.

There are usually three well-known methods to detect DM particles: using particle accelerators [4], direct detecting of scattering cross section by terrestrial detectors (CDMS II, CRESST, and CoGeNT), and indirect detecting of products from DM particle annihilation in the galactic halo [5]. The latest experimental results are not conclusive. The data from DAMA/LIBRA [6], CoGeNT [7, 8], and CRESST-II [9] experiments may imply the light DM particle with the mass around $8 - 10 \text{ GeV}$,

* wzjiang@seu.edu.cn

while other experiments such as CDMS-II [10], SIMPLE [11] and XENON10/100 [12, 13] reported null results at the same region. It's suggested that isospin-violating DM would relax the tensions between the results of DAMA, CoGeNT and XENON experiments [14]. But the possible tensions between some experiments such as those between DAMA and SIMPLE are unlikely to be affected by isospin-violating interactions.

One indirect method that is gaining attention in recent years is to study the DM effects on compact stars. On one hand, the large baryonic density in compact stars increases the probability of DM capture within the star and eventually results in gravitational trapping [15, 16]. The DM accumulation inside stars will affect the stellar structure and even contribute to the collapse of a neutron star [17–20]. On the other hand, at the later evolution period, neutron stars can be rather cold due to lack of possible burning or heating mechanisms, and therefore the heating effect by possible DM annihilation is favorable and possibly observable [20]. At the same time, self-annihilation of DM in the inner regions of neutron stars may significantly affect their kinematical properties, including linear and angular momentum [21]. Therefore, it is of great significance to study the potential effects of DM on the properties of neutron stars.

The neutron star properties are intimately related to the nuclear equation of state (EOS) of asymmetric matter, while the latter consists roughly of the EOS of symmetric matter and the density dependence of the nuclear symmetry energy. In the past, great progress has been achieved to constrain the EOS of symmetric nuclear matter using terrestrial nuclear experiments for more than three decades, see, e.g. [22, 23], for a review. It is known that the EOS around normal density can be well constrained by nuclear giant monopole resonances [22], and at supra-normal densities it can be constrained by the collective flow data from high energy heavy-ion reactions [23]. Stringent constraints on the nuclear EOS are indispensable to portray neutron stars. For instance, the maximum mass of neutron stars is mainly determined by the high-density EOS of symmetric nuclear matter. Recently, several neutron stars with large masses around $2M_{\odot}$ have been observed [24–28]. In particular, the $2M_{\odot}$ pulsar J1614-2230 was measured rather accurately through the Shapiro delay [27], and it was reported most recently that the accurate measurement of $2M_{\odot}$ pulsar J0348+0432 would be more restrictive [28]. These observations can provide astrophysical constraints on the high-density nuclear EOS. On the other hand, the density dependence of the symmetry energy that affects mostly the radius of NS's is still not well determined especially at high densities, though in the past great endeavors have been made to constrain it in the terrestrial laboratories, e.g. see Ref. [29]. Since neutron stars are natural laboratories for the exploration of baryonic matter under extreme conditions, it is hopeful to constrain the nuclear EOS of asymmetric matter at densities of interest jointly using the radius and mass observations of neutron stars [30, 31]. One should, however, note that

such constraints can not provide detailed information of the neutron star compositions or interplay between them. As far as the DM is concerned, it is rather interesting to explore many relevant issues of DM, such as its accretion onto neutron stars, interplay between normal matter (NM) and DM, interactions among DM, its effect on properties of neutron stars, and so on.

The dark-matter admixed neutron stars (DANSs) have been studied recently in several articles [20, 32–36]. Regarding DM as Fermi-gas-like matter, Li et. al. [32] provided an equal admixture of DM and NM in DANSs by taking the total pressure (energy density) as the simple sum of those of the DM and NM. Sandin and Ciarcelluti [33, 34] considered the mirror DM and assumed that neutron stars with a DM core are inherently two-fluid systems where the NM and DM couple essentially only through gravity. By varying the relative size of the DM core, they may reproduce all astrophysical mass measurements based on one nuclear matter EOS. Leung et al. [35] used the general relativistic two-fluid formalism to study the various structures of DANS. Following the approach used by Sandin and Ciarcelluti [33, 34], we consider in this work a broad variety of DM with various masses and interactions in neutron stars and examine the effects of DM on static properties of neutron stars. The paper is organized as follows. In Sec. II, we present briefly the formalism of DM based on the Lagrangian of the relativistic mean-field models as well as the formalism of two-fluid model for neutron stars. In Sec. III, numerical results and discussions are presented. At last, a summary is given in Sec. IV.

II. FORMALISM

In the RMF approach, the nucleon-nucleon interaction is usually described via the exchange of three mesons: the isoscalar meson σ , which provides the medium-range attraction between the nucleons, the isoscalar-vector meson ω , which offers the short-range repulsion, and the isovector-vector meson b_0 , which accounts for the isospin dependence of the nuclear force. The relativistic Lagrangian can be written as:

$$\begin{aligned} \mathcal{L} = & \bar{\psi}[i\gamma_\mu\partial^\mu - M + g_\sigma\sigma - g_\omega\gamma_\mu\omega^\mu - g_\rho\gamma_\mu\tau_3b_0^\mu]\psi \\ & - \frac{1}{4}F_{\mu\nu}F^{\mu\nu} + \frac{1}{2}m_\omega^2\omega_\mu\omega^\mu - \frac{1}{4}B_{\mu\nu}B^{\mu\nu} + \frac{1}{2}m_\rho^2b_{0\mu}b_0^\mu \\ & + \frac{1}{2}(\partial_\mu\sigma\partial^\mu\sigma - m_\sigma^2\sigma^2) + U_{\text{eff}}(\sigma, \omega^\mu, b_0^\mu). \end{aligned} \quad (1)$$

where $\psi, \sigma, \omega, b_0$ are the fields of the nucleon, isoscalar, isoscalar-vector, and neutral isovector-vector mesons, with their masses M, m_σ, m_ω , and m_ρ , respectively. $g_i (i = \sigma, \omega, \rho)$ are the corresponding meson-nucleon couplings. $F_{\mu\nu}$ and $B_{\mu\nu}$ are the strength tensors of ω and ρ mesons respectively,

$$F_{\mu\nu} = \partial_\mu\omega_\nu - \partial_\nu\omega_\mu, \quad B_{\mu\nu} = \partial_\mu b_{0\nu} - \partial_\nu b_{0\mu}. \quad (2)$$

The self-interacting terms of σ , ω mesons and the isoscalar-isovector coupling are given generally as

$$U_{\text{eff}}(\sigma, \omega^\mu, b_0^\mu) = -\frac{1}{3}g_2\sigma^3 - \frac{1}{4}g_3\sigma^4 + \frac{1}{4}c_3(\omega_\mu\omega^\mu)^2 + 4\Lambda_V g_\rho^2 g_\omega^2 \omega_\mu\omega^\mu b_{0\nu}b^{0\nu}. \quad (3)$$

With these nonlinear meson self-interaction terms, the models are usually known as the nonlinear models. In the relativistic mean-field (RMF) approximation, the energy density ε and pressure p are written as:

$$\begin{aligned} \varepsilon = & \sum_{i=p,n} \frac{2}{(2\pi)^3} \int^{k_{F_i}} d^3k E^* + \frac{1}{2}m_\omega^2\omega_0^2 + \frac{1}{2}m_\sigma^2\sigma_0^2 + \frac{1}{2}m_\rho^2b_0^2 \\ & + \frac{1}{3}g_2\sigma_0^3 + \frac{1}{4}g_3\sigma_0^4 + \frac{3}{4}c_3\omega_0^4 + 12\Lambda_V g_\rho^2 g_\omega^2 \omega_0^2 b_0^2, \end{aligned} \quad (4)$$

$$\begin{aligned} p = & \frac{1}{3} \sum_{i=p,n} \frac{2}{(2\pi)^3} \int^{k_{F_i}} d^3k \frac{\mathbf{k}^2}{E^*} + \frac{1}{2}m_\omega^2\omega_0^2 - \frac{1}{2}m_\sigma^2\sigma_0^2 + \frac{1}{2}m_\rho^2b_0^2 \\ & - \frac{1}{3}g_2\sigma_0^3 - \frac{1}{4}g_3\sigma_0^4 + \frac{1}{4}c_3\omega_0^4 + 4\Lambda_V g_\rho^2 g_\omega^2 \omega_0^2 b_0^2, \end{aligned} \quad (5)$$

where σ_0 , ω_0 , and b_0 are the scalar, vector, and isovector-vector fields in the mean-field approximation, respectively, $E^* = \sqrt{\mathbf{k}^2 + (M^*)^2}$, and k_F is the Fermi momentum.

In this work, we also invoke density-dependent RMF models SLC and SLCd proposed by Jiang et. al. based on the Brown-Rho scalings [37, 38]. In these density-dependent RMF models, there are no nonlinear meson self-interaction terms, and the energy density and pressure are given as

$$\varepsilon = \frac{1}{2}C_\omega^2\rho^2 + \frac{1}{2}C_\rho^2\rho^2\delta^2 + \frac{1}{2}\tilde{C}_\sigma^2(M - M^*)^2 + \sum_{i=p,n} \frac{2}{(2\pi)^3} \int_0^{k_{F_i}} d^3k E^*, \quad (6)$$

$$p = \frac{1}{2}C_\omega^2\rho^2 + \frac{1}{2}C_\rho^2\rho^2\delta^2 - \frac{1}{2}\tilde{C}_\sigma^2(M - M^*)^2 - \Sigma_0\rho + \frac{1}{3} \sum_{i=p,n} \frac{2}{(2\pi)^3} \int_0^{k_{F_i}} d^3k \frac{\mathbf{k}^2}{E^*} \quad (7)$$

where $C_\omega = g_\omega^*/m_\omega^*$, $C_\rho = g_\rho^*/m_\rho^*$, $\tilde{C}_\sigma = m_\sigma^*/g_\sigma^*$, $M^* = M - g_\sigma^*\sigma_0$ is the effective mass of nucleon, $\delta = (\rho_n - \rho_p)/\rho$ is the isospin asymmetry with ρ being the total number density of nucleons, and Σ_0 is the rearrangement term due to the density dependence of the parameters. Here, the meson coupling constants and hadron masses with asterisks denote the density dependence, given by the BR scaling.

Given above is the formalism for nuclear matter without considering the β equilibrium. For asymmetric nuclear matter at β equilibrium, the chemical equilibrium and charge neutrality conditions need to be additionally considered, which are written as:

$$\mu_n = \mu_p + \mu_e, \quad (8)$$

$$\rho_e = \rho_p, \quad (9)$$

$$\rho = \rho_n + \rho_p. \quad (10)$$

where ρ_e is the number density of electrons, and μ_n, μ_p and μ_e are the chemical potential of neutron,

proton and electron, respectively. For neutron star matter, we need also to include the contribution of the free electron gas in Eqs.(4), (5), (6) and (7).

We regard DM candidates as fermions, and assume that a neutral scalar meson couples to the DM candidate through $g_s \bar{\psi}_D \psi_D \phi$ and that a neutral vector meson couples to the conserved DM current through $g_v \bar{\psi}_D \gamma_\mu \psi_D V^\mu$. This modelling of the interactions is rather universal according to the covariance, and it's an extension of those used in Ref. [39]. Similar to the potential for baryons [40], the meson exchange gives rise to an effective potential for DM candidates:

$$V_{eff}(r) = \frac{g_v^2}{4\pi} \frac{e^{-m_v r}}{r} - \frac{g_s^2}{4\pi} \frac{e^{-m_s r}}{r}. \quad (11)$$

With appropriate coupling constants and masses, the above potential is attractive at large separations and repulsive at short distances.

The Lagrangian density for the present DM model can be written as:

$$\begin{aligned} \mathcal{L}_D = & \bar{\psi}_D [\gamma_\mu (i\partial^\mu - g_\mu V^\mu) - (M_D - g_s \phi)] \psi_D + \frac{1}{2} (\partial_\mu \phi \partial^\mu \phi - m_s^2 \phi^2) \\ & - \frac{1}{4} D_{\mu\nu} D^{\mu\nu} + \frac{1}{2} m_v^2 V_\mu V^\mu \end{aligned} \quad (12)$$

where $D_{\mu\nu}$ is the strength tensor of *vector* meson

$$D_{\mu\nu} = \partial_\mu V_\nu - \partial_\nu V_\mu.$$

The relativistic quantum field theory generated by this Lorentz-invariant \mathcal{L}_D is renormalizable, for it is similar to the massive QED with a conserved current and an additional scalar interaction.

The energy density and pressure of DM are given as:

$$\varepsilon_D = \frac{2}{(2\pi)^3} \int^{k_{FD}} d^3k \sqrt{\mathbf{k}^2 + (M_D^*)^2} + \frac{g_v^2}{2m_v^2} \rho_D^2 + \frac{m_s^2}{2g_s^2} (M_D - M_D^*)^2, \quad (13)$$

$$p_D = \frac{1}{3} \frac{2}{(2\pi)^3} \int^{k_{FD}} d^3k \frac{\mathbf{k}^2}{\sqrt{\mathbf{k}^2 + (M_D^*)^2}} + \frac{g_v^2}{2m_v^2} \rho_D^2 - \frac{m_s^2}{2g_s^2} (M_D - M_D^*)^2, \quad (14)$$

where ρ_D is the number density of DM, M_D is the mass of the DM candidate, M_D^* is the effective mass of DM determined by $M_D^* = M_D - g_s \phi_0$ with ϕ_0 being the RMF scalar field.

To study properties of the DANS, we necessarily adopt the two-fluid formulism for NM and DM between which only the gravitation exists. For a static and spherically symmetric space-time $d\tau^2 = e^{2\nu(r)} dt^2 - e^{2\lambda(r)} dr^2 - r^2 (d\theta^2 + \sin^2 \theta d\phi^2)$. The two-fluid Tolman-Oppenheimer-Volkoff (TOV) equations for the DANS are given as [34] (units are chosen such that $G = c = 1$)

$$\begin{aligned} \frac{d\nu}{dr} &= \frac{M(r) + 4\pi r^3 p(r)}{r[r - 2M(r)]}, \\ \frac{dp_N}{dr} &= -[p_N(r) + \varepsilon_N(r)] \frac{d\nu}{dr}, \\ \frac{dp_D}{dr} &= -[p_D(r) + \varepsilon_D(r)] \frac{d\nu}{dr}, \end{aligned} \quad (15)$$

where r is the radial coordinate from the center of the star, $p_N(r)$ [$p_D(r)$] and $\varepsilon_N(r)$ [$\varepsilon_D(r)$] are the pressure and energy density of NM [DM] at position r . $p(r) = p_N(r) + p_D(r)$ is the sum of the pressures at the position r , while $M(r) = \int^r d\tilde{r} 4\pi\tilde{r}^2 (\varepsilon_N(\tilde{r}) + \varepsilon_D(\tilde{r}))$ is the sum of masses contained in the sphere of the radius r . Here, the separate relations for the pressure of normal and dark matter accord with the assumption that there is no interaction between normal and dark matter except the gravitational interaction that modifies the metric together. Specifically, Eq.(15) can be deduced from the stationary condition of the star mass, that is, the variation of total star mass should vanish with respect to the variations of the energy and particle densities of normal and dark matter. The detailed derivation of Eq.(15) is given in Appendix A.

The total radius R and mass $M(R)$ of a DANS are determined by the condition $p(R) = 0$. On the other hand, we can obtain the radius and mass individually for DM and NM according to the conditions $p_N(R_N) = 0$ and $p_D(R_D) = 0$. Because NM in a DANS, consisting of neutrons, protons, and electrons (npe) at β equilibrium in this work, undergoes a phase transition from the homogeneous matter to the inhomogeneous matter at the low density region, the RMF EOS obtained from the homogeneous matter can not apply to the low density region. For a thorough description of the NM part in DANs, we thus adopt the empirical low-density EOS in the literature [41, 42], while for the DM part, no similar treatment is considered at the surface.

III. NUMERICAL RESULTS AND DISCUSSIONS

In the universe, DM has been proposed to explain the mass discrepancies according to the observed galactic rotation velocities. The latest data indicate that DM occupies about 26.8% of the total, while the ordinary visible matter only has the proportion of 4.9% and the leftover is the Dark energy. For DM as the majority of matter, people have gained few information of its mass and interaction strength. Except for the gravitational effect, the astrophysical objects composed of DM are regarded to be too faint to be detectable. DM can be possibly accreted in neutron stars by losing its energy through repeated scatterings in the high-density medium, while the practical amount of dark matter accreted onto normal neutron stars should depend on the dark matter-baryon cross section and the age of the neutron star [15, 16]. Probably, the accretion of DM can become easier if the DM that already resides in stars has necessary self-interaction. On the other hand, since the majority of matter is DM in our universe, one can imagine the existence of a large number of the massive objects composed of DM in our universe. Similar accretion of NM can take place in those DM stars. In the present work, we thus assume the DM fraction in neutron stars as an arbitrary quantity, regardless of accretion details. Similar to that in Ref. [39], here we consider DM candidates with various masses and interaction strengthes in compact stars. Though the present consideration turns out to

be somehow unconstrained, we are actually interested in possible constraints for DM by examining the its effects on the neutron star radius and mass, including the maximum mass.

For NM, we adopt the nuclear EOS with the density-dependent RMF models SLC and SLCd [37, 38]. Because the unique difference between the models SLC and SLCd is that the latter has a softer symmetry energy than the former, we may investigate the symmetry energy effect on neutron stars involving the DM. For comparisons, we also perform calculations with the nonlinear RMF model IU-FSU [43]. Parameters and saturation properties of these RMF models are listed in Table I.

TABLE I: Parameters and saturation properties for various RMF models. For the density-dependent models SLC and SLCd, tabulated are the parameters at zero density, while the parameters scaling the density dependence can be found in Ref. [38] and are not listed here. Meson masses, incompressibility and symmetry energy are in units of MeV, and the density is in unit of fm^{-3} .

	g_σ	g_ω	g_ρ	m_σ	m_ω	m_ρ	g_2	g_3	c_3	Λ_v	ρ_0	κ	E_{sym}
SLC	10.141	10.326	3.802	590.000	783.000	770	-	-	-	-	0.16	230	31.6
SLCd	10.141	10.326	5.776	590.000	783.000	770	-	-	-	-	0.16	230	31.6
IU-FSU	9.971	13.032	6.795	508.194	782.501	763	8.493	0.488	144.219	0.046	0.155	231.2	31.3

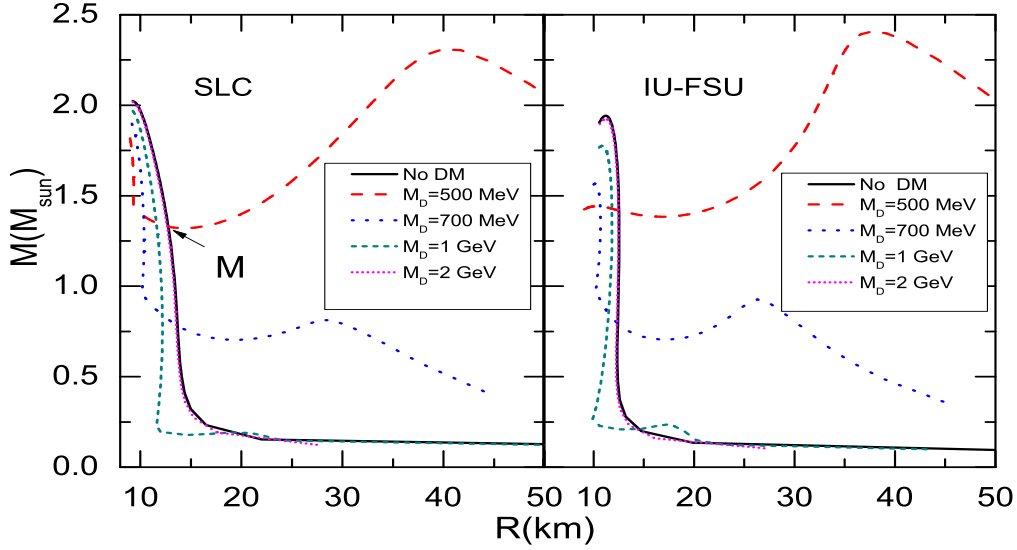


FIG. 1: (Color online) Mass-radius relations of the DANs with the DM candidate mass (M_D) ranging from 500 MeV to 2 GeV. The results in the left and right panels are obtained with the SLC and IU-FSU, respectively.

Here, the central energy density of DM and NM is assumed to be the same. Yet, we have no preference to use this unitary ratio at the neutron star center. Later on, we will come back to this point to see the effect by changing this ratio. Even if the unitary ratio at the neutron star center is used, the actual admixture of DM and NM in DANs is determined by the two-fluid TOV equations and thus is not equal at all. Shown in Fig. 1 are the Mass-radius relations for two models with the inclusion of different kinds of free DM particles that differ in masses. It is seen clearly that if the mass of the DM candidate is much larger, e.g. $\geq 2 GeV$, DM has little impact on the

Mass-radius relations of DANs. If the mass of DM is small (e.g. 500MeV), it can influence the mass-radius relations of DANs significantly. In this case, the minimum mass we obtain is found to be too heavy ($M \geq 1.32M_{\odot}$ for SLC and $M \geq 1.38M_{\odot}$ for IU-FSU) to explain the low-mass neutron stars observed [44–46]. However, if we relax the condition that the central energy densities are the same for NM and DM by reducing the central energy density of DM, we can obtain a much smaller minimum mass to be consistent with the observation of the low-mass neutron stars. By now, neither can we confirm the DM candidate terrestrially, nor can we know the mass of DM candidates. There could be many choices for DM candidates from lightest axions ($M \sim \mu\text{eV} - 10\text{meV}$) to heaviest WIMPs ($M \sim 10\text{GeV} - \text{TeV}$) [2]. Our research implies that one can perhaps distinguish them through their impact on neutron stars. Recently, an analysis about the XENON10 data claimed that direct detection experiments can be sensitive to DM candidates with masses well below the GeV scale [12]. Our calculation indicates that the observation of neutron stars is also sensitive to the DM admixture with the DM candidate mass below the GeV scale. Note that the identification of DM with the neutron star observations also involves the details of the celestial DM distribution and accretion.

In Fig. 2, it shows the mass-radius relations of DANs for different models. Here, the mass of free DM candidate is taken to be 1 GeV. We see that the existence of DM would lower the maximum stable mass of neutron stars allowed by the corresponding EOS. The reduction of the maximum mass due to the inclusion of DM is different for different models. We see that the reduction is indeed not apparent with the models SLC and SLCd that feature a stiff EOS at high densities [37]. As shown in Fig. 2, more apparent phenomenon occurs for the shift of the neutron star radius caused by the inclusion of DM. For instance, by comparing with the neutron star and DANs that both have the mass $1.4M_{\odot}$, denoted by the straight line in Fig. 2, we see that very significant reduction of the radius arises with the inclusion of DM in neutron stars. It is of special interest to point out that the 1GeV DM candidate is possibly relevant to the mirror particle of visible nucleonic matter [34, 47, 48]. In Fig. 2, we also include the constraints of mass-radius for $r_{ph} \gg R$ obtained by Steiner et al.[30]. We see that the inclusion of DM can lead to a more vertical shape, which is favorable for models SLC and SLCd to be consistent with observational constraints. Based on the general understanding of neutron star properties, the slope of the nuclear symmetry energy at normal density was extracted to be in the range 36–55 MeV at the 95% confidence level [49]. Were DM to be present in neutron stars, the astrophysical extraction of the symmetry energy should suffer significant modification due to the distinct effects induced by DM. On the other hand, though the inclusion of dark matter favors the vertical shape and smaller radius, we should point out that the comparison with the constraints obtained by Steiner et al. does not seem to be direct since such constraints were extracted using the

one-fluid TOV equation.

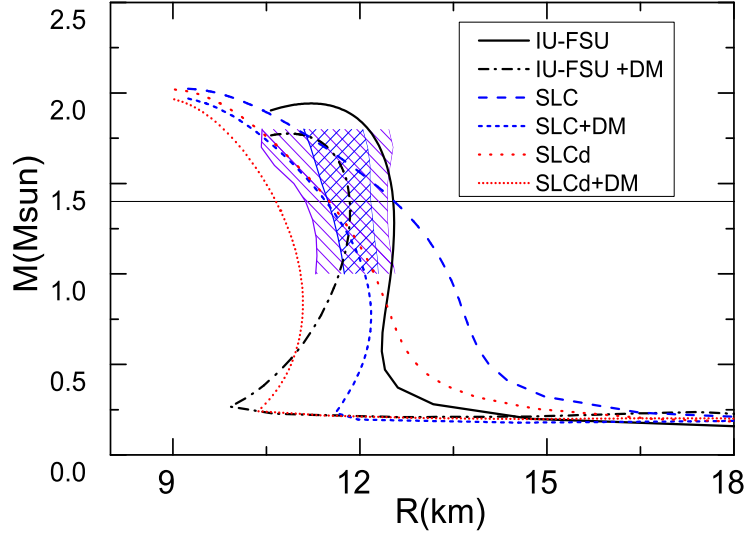


FIG. 2: (Color online) Mass-radius relations of neutron stars and DANSs for different models. In the legend, the RMF models without the suffix DM represent results of normal neutron stars, while the ones with the suffix DM stands for results of DANSs. The hatched areas give the probability distributions with 1σ (blue) and 2σ (violet) confidence limits for $r_{ph} \gg R$ summarized in Ref. [30].

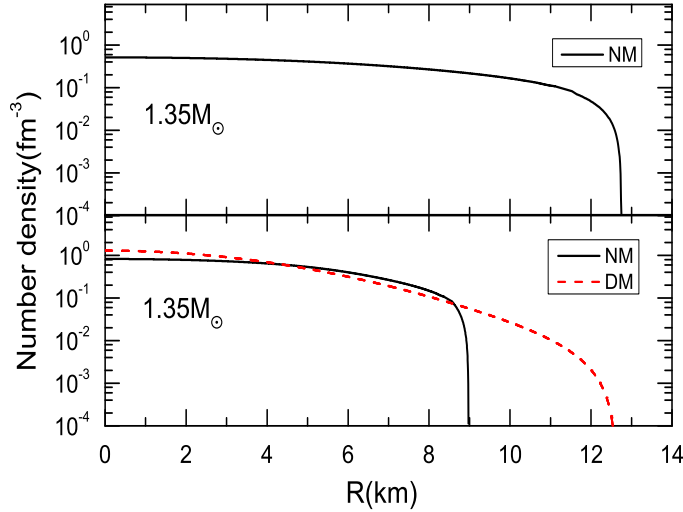


FIG. 3: (Color online) Density profiles in the neutron star and DANS that have the same mass $1.35M_\odot$ and radius (12.76km). For the DANS, the DM candidate mass is 0.5 GeV. The mass and radius setup corresponds to the point marked by M in Fig.1. The upper panel is for the normal neutron star, and the lower panel is for the DANS.

Given the appreciable DM effect on the neutron star radius, it is interesting to compare and examine various matter distributions in neutron stars and DANS. For this aim, we choose the neutron star and DANS that have the same mass and radius. The neutron star marked by M, as shown in Fig. 1, is the exact one that meets the criterion. The intersection point M corresponds for the neutron star and DANS to the mass ($1.35M_\odot$) and R (12.76km), while here the mass of DM candidate is

0.5 GeV. The number density profiles with the SLC are displayed in Fig. 3: the upper panel for the normal neutron star and the lower panel for the DANS. Significant difference in the density profiles in the neutron star and DANS can be observed. In the DANS, we see that a smaller NM core ($R \sim 9\text{km}$) is surrounded by a DM halo. Since the two stars have the same mass, it seems impossible to distinguish them only by their gravitational effects on other neighboring stellar objects. However, their visible radii are different. Thus, it is possible to distinguish them by measuring the gravitational redshift of spectral lines. In fact, the radius of the neutron star is 12.76 km, while the visible radius (namely the radius of the NM core) of the DANS is 9 km. According to the gravitational redshift formula: $z = \frac{1}{\sqrt{1-2GM/Rc^2}} - 1$, the redshift of the neutron star is obtained to be 0.206, and it is 0.340 for the DANS.

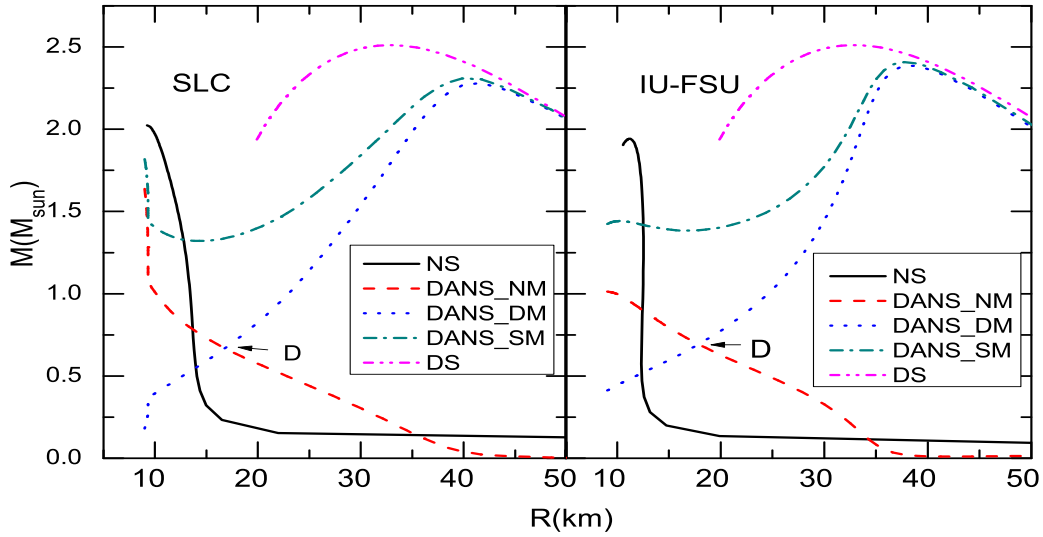


FIG. 4: (Color online) Constituent masses in the DANS with the DM particle mass being 0.5 GeV. DANS_NM (DANS_DM) is for the mass-radius relation of NM (DM) in DANS, and DANS_SM corresponds to the total one. Besides, curves for normal neutron star and pure DM star (DS) are depicted.

In order to further study the behavior shown in Fig. 1, we depict the mass-radius relations of DM and NM in Fig. 4. Here, the mass of DM candidate is again chosen to be 0.5 GeV, and the ratio of the central DM energy density to that of NM is fixed to be equal. It's obvious that with the increase of the radius, the mass proportion of NM in DANSs decreases, while the mass proportion of DM in DANSs increases. The reason for this phenomenon lies in the fact that in the current two-fluid model DM particles interact with NM particles only through the gravity. Both DM and NM produce their own maximum masses and corresponding radii. For neutron stars without DM, the maximum mass is $2.02M_\odot$ ($1.94M_\odot$) and the corresponding radius is 9.24km (11.21km) with the SLC (IU-FSU). With the inclusion of DM, the original maximum mass with the SLC (IU-FSU) is reduced to $1.82M_\odot$ ($1.44M_\odot$), and corresponding radius is decreased to 8.98km (10.3km). At the

same time, for pure DM star, the maximum mass is determined by $M_{max} = 0.627M_{\odot}(\frac{1GeV}{M_D})^2$ and corresponding radius is $R_D = 8.115km(\frac{1GeV}{M_D})^2$ [39]. By substituting $M_D = 0.5GeV$, we get the maximum mass $2.5 M_{\odot}$ and corresponding radius 32.46km. When the DM admixture starts to take place, the maximum mass and corresponding radius will be changed, as shown in Fig. 4. At the cross point (marked by D), the mass proportions of DM and NM in the DANS are equal. As the star radius continues to increase, the mass proportion of DM will be larger than that of NM, eventually leading to DM-dominant stars.

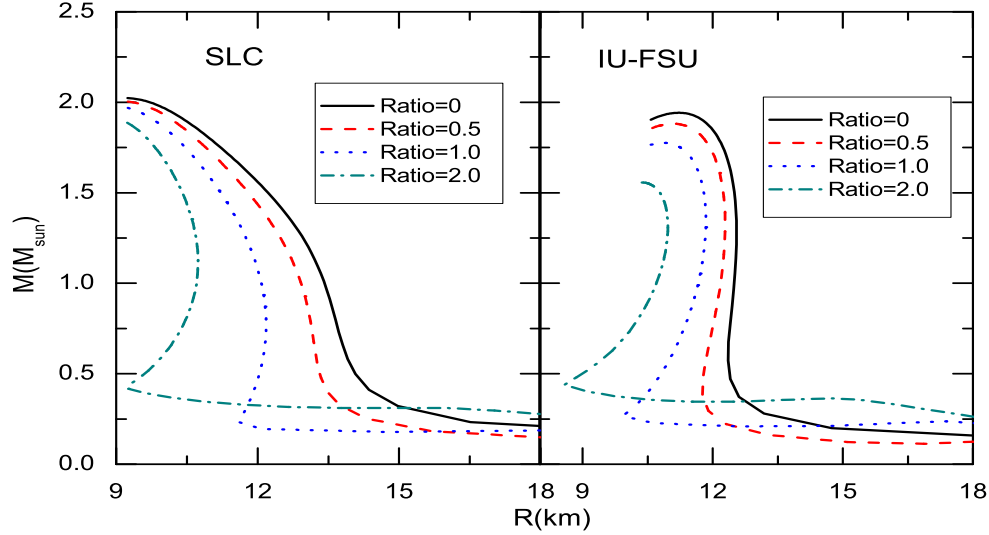


FIG. 5: (Color online) Mass-radius relations for various DM proportions. The Ratio parameter is the central energy density ratio of the DM to the NM. The zero ratio means DM-free normal neutron star.

Shown in Fig. 5 are the mass-radius relations of DANSs for various proportions of DM. Here, the mass of the DM candidate is taken to be $M_D = 1GeV$. We see that with increasing the DM ratio, the maximum mass and corresponding radius of DANS decrease. At the same time, the minimum mass of DANS increases. Similar to results shown in previous figures, the reduction of maximum mass in SLC is much less appreciable than that in IU-FSU. It is seen that the structure of DANSs is dependent on the amount of DM, and this results in a spread of mass-radius relations that cannot be interpreted with a unique equilibrium sequence.

Generally speaking, the amount of DM in DANSs is expected to vary and depends on the whole history of the star [15, 16], especially on the environment from which it originates and in which it lives. In fact, the capture of DM is difficult both because of their low reaction cross section (typically about $10^{-44}cm^2$ [50]) and the low average density of matter in the universe. But NM galaxy and galaxy clusters could act as a whole to capture DM, and enable the density of DM in some section to be high enough to produce observable signals. Actually, most evidences of DM come from these observations [51–53]. Recently, a research claimed that neutron stars in binary systems

might increase the probability to accumulate the DM [54]. Besides, neutron star could capture enough DM due to its high density [55]. Though the DM is usually assumed to be collisionless, the assumption of self-interacting DM can not be simply ruled out [56]. Even though the majority of DM is regarded to be cold and collisionless, Fan et. al. proposed most recently that a subdominant fraction of DM could have much stronger interactions [57]. In the following, we consider DM that features interactions.

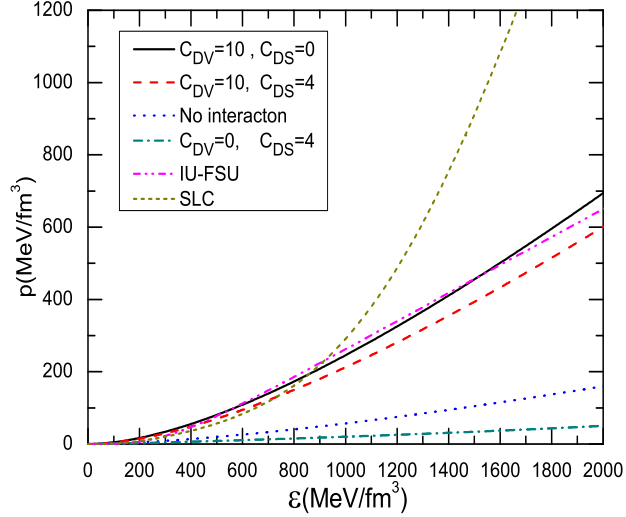


FIG. 6: (Color online) Pressure and energy density relationship of DM. The interactions with various strengthes are considered. The units of c_{DV} and c_{DS} are GeV^{-1} . For comparisons, the results of NM with the SLC and IU-FSU are also displayed.

Now, we examine the EOS with various interactions for DM. From Eqs.(13) and (14), we know that the repulsion (attraction) potential is just determined by the ratio parameter $C_{DV} = g_v/m_v$ ($C_{DS} = g_s/m_s$) in the RMF approximation. Thus, these ratio parameters can represent the interaction strength. In order to force the potential in Eq.(11) attractive at large separations and repulsive at short distances, m_v must be greater than m_s , and g_v must be greater than g_s . However, there are no limits on the size of C_{DV} and C_{DS} . Note that C_{DS} should not be too large. Otherwise, the pressure may become negative and then be not a monotonous function of energy density, invalidating the use of the TOV equation. The strengthes we select here are a little arbitrary, but this does not keep us from drawing a rough conclusion concerning the DM interaction. Shown in Fig. 6 is the pressure-energy density relationship of DM. Here, the free DM particle mass is taken as 1GeV, and we choose $C_{DV} = 10GeV^{-1}$ and/or $C_{DV} = 4GeV^{-1}$ in the calculation. It is seen in Fig. 6 that the repulsion with a large C_{DV} stiffens clearly the EOS of DM, while attraction just softens moderately the EOS of DM because of a much smaller C_{DS} . For comparisons, we also depict the NM results with the SLC and IU-FSU in Fig. 6.

With various DM EOSs, we display the mass-radius relation in Fig.7. Because the repulsion

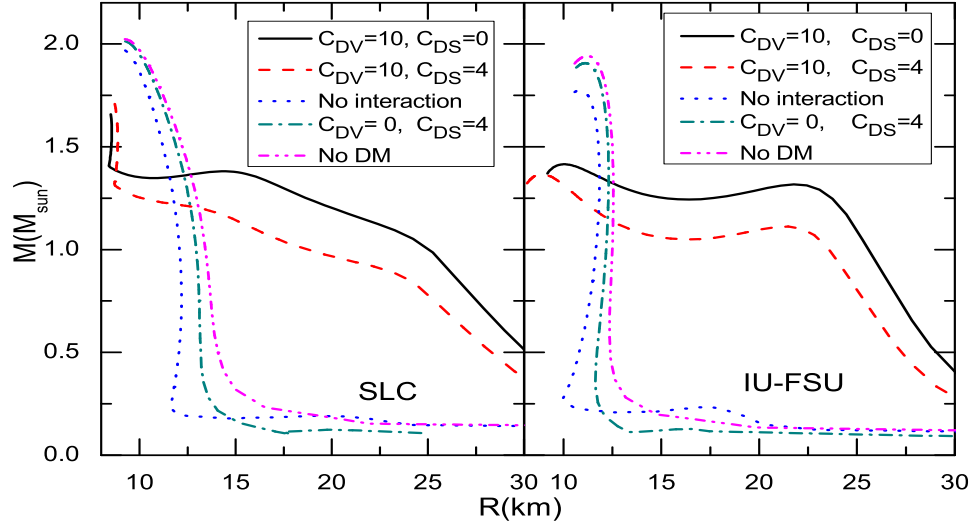


FIG. 7: (Color online) Mass-radius relations with various DM EOSs. The attractive and/or repulsive strengths are labelled in the legend.

provides resistance to the gravitational attraction, in principle, the more the repulsion, the heavier the star. In the one-fluid model, this is simply right. However, in the two-fluid model, the mass-radius relation is not so simple. Because of the gravity provided by the other fluid, the maximum mass of each fluidic constituent reduces, while the repulsion added by the DM just increases the maximum mass of the DM constituent. This can be clearly observed by comparing the results of solid and red-dashed curves in Fig. 7. In the case of the pure attraction for DM, we see that the mass-radius relation is just modified moderately, because the attraction diminishes the DM proportion in the star. It's obvious that the stiffer the EOS of DM shown in Fig. 6, the more effect it could have on the mass-radius relation of DANs. Though the maximum mass of neutron stars is here less than $2M_{\odot}$ with the given repulsion for DM, it can exceed $2M_{\odot}$ for stronger repulsion. Note that though these statements are made from the results obtained with the specific mass of DM candidate, it is qualitatively valid for other choices of the DM candidate mass.

While the interaction of DM leads to various mass-radius relations, it is interesting to investigate constituent density profiles in DANs. Shown in Fig. 8 are various particle number density profiles for the DANs with the DM interactions corresponding to those in Figs. 6 and 7. Here, the central energy density is fixed to be $600 \text{ MeV}/fm^3$ for both NM and DM. In this case, the mass of the DAN ranges from $1.13M_{\odot}$ to $1.38M_{\odot}$ and from $1.34M_{\odot}$ to $1.60M_{\odot}$ for the SLC and IU-FSU, respectively. We can observe that the attraction of DM shrinks the DM density distribution, leading to the increase of the number density gradient of DM in the DAN, together with the decrease of the number density gradient of NM. The repulsion supports an spatial extension, opposite to the shrinkage provided by the attraction. The DM extension out of NM actually generates a clear DM halo. It is seen from Fig. 8

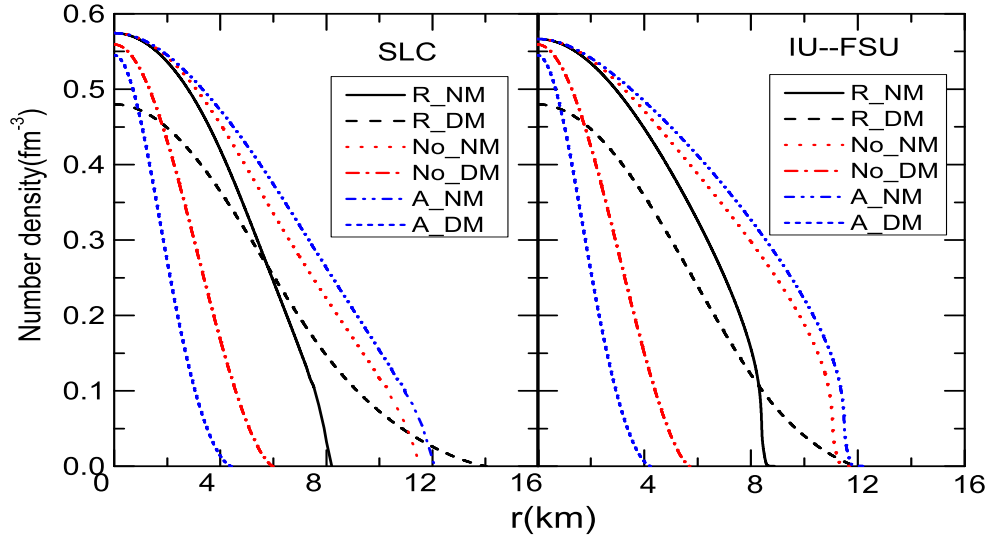


FIG. 8: (Color online) Number density profiles in DANSs. In the legend, R (A) represents the pure repulsion (attraction) with the interaction strength $C_{DV} = 10\text{GeV}^{-1}$, $C_{DS} = 0$ ($C_{DV} = 0$, $C_{DS} = 4\text{GeV}^{-1}$), while No represents no interaction for DM. These cases are corresponding to those in Figs.6 and 7.

that the number density of the DM halo is much larger than that shown in Fig.3. Our calculation also indicates that it's more likely to form the DM halo with a lower central energy density. The halo structure is somehow dependent on nuclear EOS, as shown in Fig. 8. This is because various EOSs provide different NM distribution that screens DM. Though DM halo is invisible, the visible size of DANSs is now certainly affected by the interaction of DM. We can address that the visible radius of DANSs is not only affected by the DM proportion, but also affected by the interaction of DM. This would affect the extraction of EOS from astrophysical observations.

TABLE II: The allowed amount of the DM accreted onto the normal neutron star due to the equilibrium between the gravity and matter pressure. The normal neutron star mass is fixed to be $1.30M_{\odot}$. ε_c is the central energy density which is equal for DM and NM, and R_{DM} (R_{NM}) and M_{DM}/M_{\odot} (M_{NM}/M_{\odot}) are the respective radius and mass in DANSs. The energy density and radius are in units of $\text{MeV}/\text{fm}^{-3}$ and km , respectively. The interaction type in the first column stands for the various interaction strengths of DM that are the same as the corresponding cases in Fig.8.

	Model	ε_c	R_{DM}	M_{DM}/M_{\odot}	R_{NM}	M_{NM}/M_{\odot}	M_{SM}/M_{\odot}
No DM	SLC	508	-	-	12.85	1.30	1.30
	SLCd	621	-	-	11.75	1.30	1.30
Attraction	SLC	620	4.56	0.03	12.40	1.30	1.33
	SLCd	725	4.24	0.03	11.39	1.30	1.33
No interaction	SLC	820	5.36	0.10	11.46	1.30	1.40
	SLCd	900	5.12	0.10	10.67	1.30	1.40
Repulsion	SLC	1800	6.26	0.34	8.53	1.30	1.64
	SLCd	1776	6.25	0.33	8.31	1.30	1.63

The DANS mass varies with the interaction of DM at given central energy density. By varying the interaction of DM, we may obtain the different DM proportion in the DANS according to the mechanical equilibrium between the gravity and matter pressure. Specifically, we consider the example

that the mass from constituent NM is fixed to be $1.30M_{\odot}$. The results are tabulated in Table II. Here, the interaction strengthes of DM are the same as the corresponding cases in Fig. 8, and the central energy density of NM and DM is set to be equal. From Table II, we see that the DM amount in the neutron star, allowed by the mechanical equilibrium, causes the increase of the ε_c of the star. The stiffer the EOS of DM, the greater the ε_c . Indeed, the allowed DM amount accumulated in the DANS is the maximum DM amount beyond which the DANS should collapse into the black hole. The observation from Table II indicates that the maximum mass of the DANS increases surely by changing the interaction from the attraction to repulsion. We may thus speculate that the DANS maximum mass further increases to exceed the $2M_{\odot}$ restriction [27, 28] by increasing the repulsion strength. This is the case that can be verified numerically. Moreover, it is interesting to point out that the excess of $2M_{\odot}$ can be realized by increasing the ratio of the DM central energy density to that of NM without changing the repulsion strength used in Table II. Nevertheless, as the DM amount in the DANS increases to provide more gravitation, NM in the DANS is more compressed and becomes more compact.

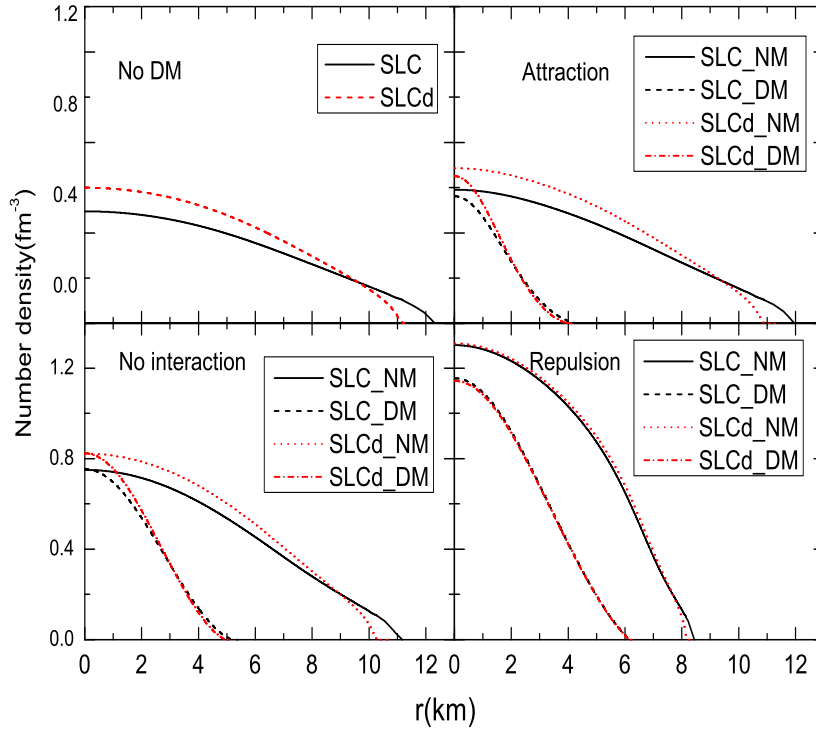


FIG. 9: (Color online) Number density profiles in the DANS with different DM interactions for models SLC and SLCd.

In Fig. 9, we plot various number density profiles for neutron stars with the masses and corresponding interactions same as those in Table II. In the present case, we see that DM resides in the

central region of DANS and no DM halo forms. We see in Fig. 9 that DM in the DANS can influence the distribution of NM. In the case without DM, we know that the different matter distribution with the SLC and SLCd is attributed to their different nuclear symmetry energy. It is interesting to see that DM in the DANS results in the decrease of the difference in the NM density profiles. Moreover, the decrease can be enhanced by stiffening the DM EOS. If appropriate repulsion is assumed to have between DM, the difference in density profiles and consequently in star radii given by the SLC and SLCd can run almost to disappear. In this case, the difference in neutron star radii turns out to be quite small, as seen in Table II. Though the models are different just in the density dependence of nuclear symmetry energy, the astrophysical extraction of the constraint on the symmetry energy seems to be difficult if the neutron star is admixed with DM featuring sufficiently strong repulsion.

IV. SUMMARY

In this work, we have studied the effects of fermionic DM on the properties of neutron stars using the two-fluid TOV formalism. While by assuming that the DM and NM have no interactions but the gravitation, we have considered various choices for masses and interactions for DM candidates. It is found that the mass-radius relationship of DANSs depends sensitively on the mass of DM candidate, the amount of DM, and interactions among DM candidates. The existence of DM in DANSs results in a spread of mass-radius relationships that cannot be interpreted with a unique equilibrium sequence. The mass region of DM candidates where DM affects significantly the DANS properties is found to be below a few GeV. An important consequence of the DM admixture in neutron stars is the shrinkage of the NM surface that actually results in the small radius observation. Interestingly, we find that the difference in density profiles in the DANS and consequently in star radii caused by various density dependencies of nuclear symmetry energy tends to disappear, as long as the repulsion of accumulated DM is sufficient. It is interesting to see that the DM distribution can surpass the NM distribution to form DM halo especially for the DM candidates with the low mass. Generally, an explicit DM halo may arise favorably if the repulsion of DM exists. These phenomena indicate that the admixture of DM in neutron stars can significantly affect the astrophysical extraction of nuclear EOS through neutron star measurements. Provided the nuclear EOS can be well determined in the terrestrial laboratory, it would be hopeful to look for the evidence for DM using the phenomena that are sensitive to the DM admixture in the neutron star observations. On the other hand, the DM admixture can affect the maximum mass of neutron stars. Though the maximum mass tends to be reduced by the DM accretion, the practical situation is not so simple and actually depends on very details of models, the DM fraction and interactions. In particular, favorably with the large DM fraction in the DANS the repulsive interaction among DM can lead to massive stars with the mass

above $2M_\odot$.

Acknowledgement

The work was supported in part by the SRTP Grant of the Educational Ministry No. 1210286047, the National Natural Science Foundation of China under Grant Nos. 10975033 and 11275048, the China Jiangsu Provincial Natural Science Foundation under Grant No.BK20131286, and the China Scholarship Council.

Appendix A: Derivation of Eq.(15)

While one can find the derivation of the one-fluid TOV equation in the literature, we give a detailed deduction of the two-fluid TOV equations [Eq.(15)] according to the stellar stability condition [58]. With the uniform entropy per particle and chemical composition for both normal matter and dark matter, the equilibrium of a particular stellar configuration reaches, if and only if the M defined by

$$M = \int_0^\infty 4\pi r^2 [\varepsilon_N(r) + \varepsilon_D(r)] dr, \quad (\text{A1})$$

is stationary with respect to all variations of $\varepsilon_N(r)$ and $\varepsilon_D(r)$ that maintain the conservation of the two qualities

$$N_D = \int_0^\infty 4\pi r^2 \rho_D(r) \left[1 - \frac{2GM(r)}{r}\right]^{-1/2} dr, \quad (\text{A2})$$

and

$$N_N = \int_0^\infty 4\pi r^2 \rho_N(r) \left[1 - \frac{2GM(r)}{r}\right]^{-1/2} dr, \quad (\text{A3})$$

and that leave the entropy per particle and the chemical composition unchanged.

We introduce two Lagrange multipliers λ and α to demonstrate the fact that M will be stationary with respect to all variations that leave N_N and N_D fixed if and only if $\delta M - \lambda \delta N_N - \alpha \delta N_D$ is stationary with respect to all variations. The functional variation for the given variation $\delta \varepsilon_N(r)$ and $\delta \varepsilon_D(r)$ can be written as

$$\begin{aligned} & \delta M - \lambda \delta N_N - \alpha \delta N_D \\ &= \int_0^\infty 4\pi r^2 [\delta \varepsilon_N(r) + \delta \varepsilon_D(r)] dr \\ &- \lambda \int_0^\infty 4\pi r^2 \left[1 - \frac{2GM(r)}{r}\right]^{-1/2} \delta \rho_N(r) dr \\ &- \lambda G \int_0^\infty 4\pi r \left[1 - \frac{2GM(r)}{r}\right]^{-3/2} \rho_N(r) \delta M(r) dr \\ &- \alpha \int_0^\infty 4\pi r^2 \left[1 - \frac{2GM(r)}{r}\right]^{-1/2} \delta \rho_D(r) dr \\ &- \alpha G \int_0^\infty 4\pi r \left[1 - \frac{2GM(r)}{r}\right]^{-3/2} \rho_D(r) \delta M(r) dr, \end{aligned} \quad (\text{A4})$$

with

$$\delta M(r) = \int_0^r 4\pi r'^2 [\delta \varepsilon_N(r') + \delta \varepsilon_D(r')] dr'. \quad (\text{A5})$$

Note that the integrands vanish outside $R + \delta R$ and we use the upper limit ∞ just for convenience.

These variations are supposed not to change the entropy per nucleon and DM particle, namely

$$\delta\left(\frac{\varepsilon_N(r)}{\rho_N(r)}\right) + p_N(r)\delta\left(\frac{1}{\rho_N(r)}\right) = 0, \quad (\text{A6})$$

$$\delta\left(\frac{\varepsilon_D(r)}{\rho_D(r)}\right) + p_D(r)\delta\left(\frac{1}{\rho_D(r)}\right) = 0, \quad (\text{A7})$$

and thus

$$\begin{aligned} \delta \rho_N(r) &= \frac{\rho_N(r)}{p_N(r) + \varepsilon_N(r)} \delta \varepsilon_N(r), \\ \delta \rho_D(r) &= \frac{\rho_D(r)}{p_D(r) + \varepsilon_D(r)} \delta \varepsilon_D(r). \end{aligned} \quad (\text{A8})$$

By substituting Eq.(A5) into Eq.(A4) and interchanging the r and r' integrals, we have

$$\begin{aligned} &\delta M - \lambda \delta N_N - \alpha \delta N_D \\ &= \int_0^\infty 4\pi r'^2 \left\{ 1 - \frac{\lambda \rho_N(r)}{p_N(r) + \varepsilon_N(r)} \left[1 - \frac{2GM(r)}{r} \right]^{-1/2} \right. \\ &\quad \left. - \lambda F_N(r) - \alpha F_D(r) \right\} \delta \varepsilon_N dr \\ &+ \int_0^\infty 4\pi r'^2 \left\{ 1 - \frac{\alpha \rho_D(r)}{p_D(r) + \varepsilon_D(r)} \left[1 - \frac{2GM(r)}{r} \right]^{-1/2} \right. \\ &\quad \left. - \lambda F_N(r) - \alpha F_D(r) \right\} \delta \varepsilon_D dr, \end{aligned} \quad (\text{A9})$$

where we have defined two quantities

$$\begin{aligned} F_N(r) &= G \int_r^\infty 4\pi r' \rho_N(r') dr' \left[1 - \frac{2GM(r')}{r'} \right]^{-3/2} dr', \\ F_D(r) &= G \int_r^\infty 4\pi r' \rho_D(r') dr' \left[1 - \frac{2GM(r')}{r'} \right]^{-3/2} dr'. \end{aligned}$$

We see that $\delta M - \lambda \delta N_N - \alpha \delta N_D$ will vanish for all $\delta \varepsilon_D(r)$ and $\delta \varepsilon_N(r)$ if and only if

$$1 - \frac{\lambda \rho_N(r)}{p_N(r) + \varepsilon_N(r)} \left[1 - \frac{2GM(r)}{r} \right]^{-1/2} - \lambda F_N - \alpha F_D = 0, \quad (\text{A10})$$

$$1 - \frac{\alpha \rho_D(r)}{p_D(r) + \varepsilon_D(r)} \left[1 - \frac{2GM(r)}{r} \right]^{-1/2} - \lambda F_N - \alpha F_D = 0, \quad (\text{A11})$$

while two equations can be rewritten as

$$\frac{\rho_N(r)}{p_N(r) + \varepsilon_N(r)} \left[1 - \frac{2GM(r)}{r} \right]^{-1/2} + F_N + \frac{\alpha}{\lambda} F_D = \frac{1}{\lambda}, \quad (\text{A12})$$

$$\frac{\rho_D(r)}{p_D(r) + \varepsilon_D(r)} \left[1 - \frac{2GM(r)}{r} \right]^{-1/2} + F_D + \frac{\lambda}{\alpha} F_N = \frac{1}{\alpha}, \quad (\text{A13})$$

with

$$\frac{\lambda}{\alpha} = \frac{\rho_D(r)[p_N(r) + \varepsilon_N(r)]}{\rho_N(r)[p_D(r) + \varepsilon_D(r)]}, \quad (\text{A14})$$

obtained by equating the left-hand sides of Eqs.(A10) and (A11). Because the right-hand side of Eqs.(A12) and (A13) is independent of the coordinate r , the differentiation over the coordinate vanishes. By differentiating both sides of Eq.(A12), we have

$$\begin{aligned} & \left\{ \frac{\rho'_N(r)}{p_N(r) + \varepsilon_N(r)} - \frac{\rho_N(r)[p'_N(r) + \varepsilon'_N(r)]}{[p_N(r) + \varepsilon_N(r)]^2} \right\} \left[1 - \frac{2GM(r)}{r} \right]^{-1/2} \\ & + \frac{G\rho_N(r)}{p_N(r) + \varepsilon_N(r)} \left\{ 4\pi r[\varepsilon_D(r) + \varepsilon_N(r)] - \frac{M(r)}{r^2} \right\} \left[1 - \frac{2GM(r)}{r} \right]^{-3/2} \\ & - 4\pi r G \rho_N(r) \left[1 - \frac{2GM(r)}{r} \right]^{-3/2} \\ & - 4\pi r G \rho_N(r) \frac{p_D(r) + \varepsilon_D(r)}{p_N(r) + \varepsilon_N(r)} \left[1 - \frac{2GM(r)}{r} \right]^{-3/2} = 0 \end{aligned} \quad (\text{A15})$$

The condition of uniform entropy per nucleon gives

$$\frac{d}{dr} \left(\frac{\varepsilon_N(r)}{\rho_N(r)} \right) + p_N \frac{d}{dr} \left(\frac{1}{\rho_N(r)} \right) = 0,$$

which leads to the relation

$$\rho'_N(r) = \frac{\rho_N(r)\varepsilon'_N(r)}{p_N(r) + \varepsilon_N(r)}. \quad (\text{A16})$$

Substituting Eq.(A16) into Eq.(A15), we get the TOV equation for normal matter

$$p'_N(r) = -G[p_N(r) + \varepsilon_N(r)] \left[1 - \frac{2GM(r)}{r} \right]^{-1} \left\{ 4\pi r[p_N(r) + p_D(r)] + \frac{M(r)}{r^2} \right\} \quad (\text{A17})$$

Similarly, we can obtain the TOV equation for dark matter as:

$$p'_D(r) = -G[p_D(r) + \varepsilon_D(r)] \left[1 - \frac{2GM(r)}{r} \right]^{-1} \left\{ 4\pi r[p_N(r) + p_D(r)] + \frac{M(r)}{r^2} \right\} \quad (\text{A18})$$

Eqs.(A17) and (A18) are exactly the TOV equations given in Eq.(15).

-
- [1] M. Roos, arXiv:1001.0316v2[astro-ph.CO].
 - [2] J. L. Feng, arXiv:1003.0904v2[astro-ph.CO].
 - [3] P. A. R. Ade et al. (Planck Collaboration), arXiv:1303.5076v1 [astro-ph.CO].
 - [4] G. Arcadi, R. Catena, P. Ullio, arXiv:1211.5129 [hep-ph].
 - [5] J. L. Feng, arXiv:1211.3116 [astro-ph.HE].
 - [6] R. Bernabei et al. (DAMA Collaboration), Eur. Phys. J. C **67**, 39 (2010).
 - [7] C. E. Aalseth et al. (CoGeNT Collaboration), Phys. Rev. Lett. **106**, 131301 (2011).
 - [8] C. E. Aalseth et al. (CoGeNT Collaboration), Phys. Rev. Lett. **107**, 141301 (2011).
 - [9] G. Angloher et al. (CRESST-II Collaboration), Eur. Phys. J. C **72**, 1971 (2012).
 - [10] Z. Ahmed et al. (CDMS-II Collaboration), Phys. Rev. Lett. **06**, 131302 (2011).
 - [11] M. Felizardo et al. (The SIMPLE Collaboration), Phys. Rev. Lett. **108**, 201302 (2012).
 - [12] R. Essig et al., Phys. Rev. Lett. **109**, 021301 (2012).
 - [13] E. Aprile et al. (XENON100 Collaboration), Phys. Rev. Lett. **109**, 181301 (2012).
 - [14] H. B. Jin, S. Miao and Y. F. Zhou, Phys. Rev. D **87**, 016012 (2013).
 - [15] I. Goldman and S. Nussinov, Phys. Rev. D **40**, 3221 (1989).
 - [16] C. Kouvaris, Phys. Rev. D **77**, 023006 (2008).
 - [17] C. Kouvaris and P. Tinyakov, Phys. Rev. Lett. **107**, 091301 (2011).
 - [18] C. Kouvaris and P. Tinyakov, Phys. Rev. D **83**, 083512 (2011).
 - [19] C. Kouvaris, Phys. Rev. Lett. **108**, 191301 (2012).
 - [20] A. D. Lavallaz, M. Fairbairn, Phys. Rev. D **81**, 123521 (2010).
 - [21] M. Ángeles, P. García, J. Silk, Phys. Lett. B **711** 6(2012).

- [22] D. H. Youngblood, H. L. Clark, and Y. W. Lui, *Phys. Rev. Lett.* **82**, 691 (1999).
- [23] P. Danielewicz, R. Lacey, W.G. Lynch, *Science* **298**, 1592, (2002).
- [24] D. J. Nice, E. M. Splaver, I. H. Stairs, O. Loehmer, et al., *Astrophys. J.* **634**, 1242 (2005).
- [25] D. J. Nice, I. H. Stairs, L. E. Kasian, 2008, in *AIP Conf. Ser.* 983, 40 Years of Pulsars: Millisecond Pulsars, Magnetars and More, ed. C. Bassa, Z.Wang, A. Cumming, and V. M. Kaspi (AIP: New York), 453.
- [26] F. Özel, *Nature* **441**, 1115 (2006).
- [27] P. B. Demorest, T. Pennucci, S. M. Ransom, M. S. E. Roberts, and J. W. T. Hessels, *Nature* **467**, 1081 (2010).
- [28] J. Antoniadis, P. C. C. Freire, N. Wex, et al. *Science*, **340**, 448 (2013).
- [29] B. A. Li, L. W. Chen, and C. M. Ko, *Phys. Rep.* **464**, 113 (2008).
- [30] A. W. Steiner, J. M. Lattimer, and E. F. Brown, *Astrophys. J.* **722**, 33 (2010).
- [31] F. Özel and D. Psaltis, *Phys. Rev. D* **80**, 103003 (2009).
- [32] A. Li, F. Huang, and R. X. Xu, *Astroparticle Phys.* **37**, 70 (2012).
- [33] F. Sandin, P. Ciarcellut, *Astroparticle Phys.* **32**, 278 (2009).
- [34] P. Ciarcellut, F. Sandin, *Phys. Lett. B* **695**, 19 (2011).
- [35] S. C. Leung, M. C. Chu, L. M. Lin, *Phys. Rev. D* **84**, 107301 (2011).
- [36] C. Kouvaris, P. Tinyakov, *Phys. Rev. D* **82**, 063531 (2010).
- [37] W. Z. Jiang, B. A. Li and L. W. Chen, *Phys. Lett. B* **653**, 184 (2007).
- [38] W. Z. Jiang, B. A. Li and L. W. Chen, *Phys. Rev. C* **76**, 054314 (2007).
- [39] G. Narain, J. schaffner-Bielich, I. N. Mishustin, *Phys. Rev. D* **74**, 063003 (2006).
- [40] A. L. Fetter and J. D. Walecka, *Quantum theory of Many-particle Systems*, (McGraw-Hill, New York, 1971).
- [41] G. Baym, C. Pethick, and P. Sutherland, *Astrophys. J.* **170**, 299 (1971).
- [42] K. Iida and K. Sato, *Astrophys. J.* **477**, 294 (1997).
- [43] F. J. Fattoyev, C. s.J. Horowitz, J. Piekarewicz, G. Shen, *Phys. Rev. C* **82**, 055803 (2010).
- [44] J. M. Lattimer and M. Prakash, *Science* **304**, 536 (2004).
- [45] M. H. van Kerkwijk, J. van Paradijs, E. J. Zuiderwijk, *Astron. Astrophys.* **303**, 497 (1995).
- [46] S. E. Thorsett, D. Chakrabarty, *Astrophys. J.* **512**, 288 (1999).
- [47] S. I. Blinnikov and M. Yu. Khlopov, *Sov. Astron.* **27**, 371 (1983).
- [48] M. Yu. Khlopov, G. M. Beskin, N. G. Bochkarev, L. A. Pustilnik and S. A. Pustilnik, *Sov. Astron.* **35**, 21 (1991).
- [49] A. W. Steiner and S. Gandolfi, *Phys. Rev. Lett.* **108**, 081102 (2012).
- [50] Z. Ahmed et al.(CDMS Collaboration). *Phys. Rev. Lett.* **102**, 011301(2009).
- [51] A. Refregier, arXiv:astro-ph/0307212.
- [52] J. A. Tyson, G. P. Kochanski, and I. P. Dell’Antonio, arXiv:astro-ph/9801193.
- [53] A. D. Lewis, D. A. Buote, and J. T. Stocke, *Astrophys. J.* **586** 135(2003).
- [54] L. Brayeur, P. Tinyakov. *Phys. Rev. Lett.* **109**, 061301 (2012).
- [55] B. C. Bromley, *Astrophys. J. Suppl. Ser.* **197**, 37 (2011), arXiv:1112.2355v1[astro-ph.HE].
- [56] D. N. Spergel and P. J. Steinhardt, *Phys. Rev. Lett.* **84**, 3760 (2000).
- [57] J. Fan, A. Katz, L. Randall, and M. Reece, *Phys. Rev. Lett.* **110**, 211302 (2013).
- [58] S. Weinberg, *Gravitation and cosmology: principles and applications of the general theory of relativity*, (Wiley, New York, 1972)